

## Multiaxial Stress-Strain Modeling and Effect of Additional Hardening due to Nonproportional Loading

G. Rashed<sup>a,\*</sup>, R. Ghajar<sup>b</sup>, G. Farrahi<sup>c</sup>

<sup>a</sup>*Ahwaz Faculty of Petroleum Engineering, Ahwaz, P.O. Box 63431, I. R. Iran*

<sup>b</sup>*Associate Professor, Department of Mechanical Engineering, K. N. Toosi University of Technology, P. O. Box 16765-3381, Tehran, I. R. Iran*

<sup>c</sup>*Associate Professor, Department of Mechanical Engineering, Sharif University of Technology, P. O. Box 11365-9567, Tehran, I. R. Iran*

(Manuscript Received June 5, 2006; Revised May 8, 2007; Accepted May 11, 2007)

---

### Abstract

Most engineering components are subjected to multiaxial rather than uniaxial cyclic loading, which causes multiaxial fatigue. The pre-requisite to predict the fatigue life of such components is to determine the multiaxial stress-strain relationship. In this paper the multiaxial cyclic stress-strain model under proportional loading is derived using the modified power law stress-strain relationship. The equivalent strain amplitude consisted of the normal strain excursion and maximum shear strain amplitude is used in the proportional model to include the additional hardening effect due to nonproportional loading. Therefore a new multiaxial cyclic stress-strain relationship is devised for out of phase nonproportional loading. The model is applied to the nonproportional loading case and the results are compared with the other researchers' experimental data published in the literature, which are in a reasonable agreement with the experimental data. The relationship presented here is convenient for the engineering applications.

*Keywords:* Multiaxial cyclic stress-strain relationship; Nonproportional; Strain excursion; Critical plane; Thin-walled tube

---

### 1. Introduction

Most engineering components and structures such as aircraft, automobile and rotary drilling rig are subjected to multiaxial rather than uniaxial cyclic loading. The design of these components requires the life prediction under both proportional and nonproportional multiaxial loading. The life prediction under such a loading condition needs stress-strain relation that must be derived from the standard uniaxial cyclic test data. The cyclic stress-strain responses under multiaxial loading, which depend on the loading path, are complex and the fatigue behavior of materials and structures is difficult to describe. The multiaxial fa-

tigue criteria are based on the reduction of the complex multiaxial loading to an equivalent uniaxial loading.

The multiaxial fatigue analysis requires the reliable models that can predict the complex elastic-plastic stress-strain behavior occurring in many cyclically loaded elements. In the last decade, various stress-strain models have been proposed that can simulate multiaxial cyclic behavior of materials. McDowell (1985) and Bannantine (1989) used a two-surface model to describe the stress-strain relation. Chu (1984) generalized Mroz's discrete yield surface field concept using a continuous field of work hardening module (Mroz, 1967).

The cyclic stress-strain relationship under uniaxial loading can be described by the modified power law equation (Chu et al., 1993), but it seems rather

---

\*Corresponding author. Tel.: +98 21 4444 2903, Fax.: +98 21 4445 5846  
E-mail address: rashed545@yahoo.com

complex for multiaxial cyclic loading case. Under multiaxial nonproportional cyclic loading, the stress depends on both the strain and the loading path that makes the situation more complicated. Under such a condition of loading the fatigue life prediction strictly depends on the accuracy of the stress-strain relationship. In the last two decades, many good theoretical and experimental works have been published, but in spite of wide emphasize on multiaxial cyclic constitutive theory the direct prediction of multiaxial fatigue life is rather complicated and rare. The complication arises from the plasticity theory approach, which requires stress-strain relation for parts subjected to prescribed cyclic loads and/or displacements. Currently, the plastic incremental models are usually used to analyse the stress-strain relationship of parts under multiaxial cyclic loading (Doong and Socie, 1991; McDowell and Socie, 1982). The simulation of the numerical calculation of the cyclic stress-strain relationship is more complicated and requires determination of many material constants. Therefore these methods have limited engineering applications.

In this paper a multiaxial cyclic stress-strain model for a thin walled tubular specimen under either proportional or nonproportional loading condition is developed. The accuracy of the model is verified against Fatemi's experimental results (Fatemi, 1989a; Fatemi, 1989b). The proposed multiaxial cyclic stress-strain relation has convenient engineering application for multiaxial fatigue life prediction.

## 2. The tension-torsion proportional and nonproportional cyclic loading of a thin-walled tube

There is no unique definition for proportional and nonproportional loading. It can be defined mechanically in terms of the rotation of principal shear strain planes. From the fatigue point of view, proportional is defined as a history that results in a fixed orientation of the principal axes associated with the alternating components of strain or as any state of time varying stress where the orientation of the principal stress axes remain fixed with respect to the axes of the component. Nonproportional loading is defined as any state of time varying stress in which the orientation of the principal stress/strain axes change with time and induces additional cyclic hardening in the material. With the same maximum shear

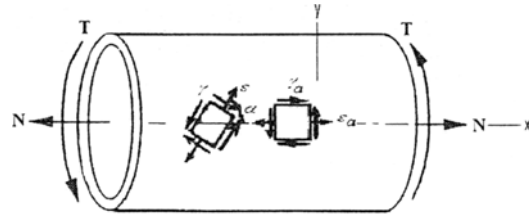


Fig. 1. A thin-walled tube specimen under tension-torsion loading.

strain range per cycle the normal stress and strain is multiplied by a factor greater than one for nonproportional loading case. This factor may even take a maximum value of two (Socie, 1993).

Let us consider a thin infinitely long circular cylinder under the loading condition shown in Fig. 1. The nominal tensile and shear stress ( $\sigma$  and  $\tau$ ) will be:

$$\sigma = \frac{4N}{\pi(D_o^2 - D_i^2)} \quad (1)$$

$$\tau = \frac{8TD}{\pi(D_o^4 - D_i^4)} \quad (2)$$

where  $D_o$  and  $D_i$  are tube outside and inside diameters, respectively.

Generally,  $\sigma$  and  $\tau$  are time-dependent, i.e.:

$$\sigma(t) = \sigma_m \pm \sigma_a f(t) \quad (3)$$

$$\tau(t) = \tau_m \pm \tau_a g(t) \quad (4)$$

where  $f(t)$  and  $g(t)$  are normalized time functions, subscripts  $m$  and  $a$  are used for mean-value and amplitude of the parameters, respectively.

Based on the above definitions the proportional and nonproportional loading are defined as:

$$\frac{\sigma(t)}{\tau(t)} = \begin{cases} \text{Cte proportional} \\ \text{Variable nonproportional} \end{cases} \quad (5)$$

## 3. Multiaxial stress-strain analysis

To describe multiaxial stress-strain behavior of the material, mathematically the new form of the modified power law equation is used here (Chu et al., 1993):

$$\begin{aligned} \frac{\Delta \varepsilon_{eq}}{2} &= \frac{\Delta \varepsilon_{eq}^e}{2} + \zeta \left( \frac{\Delta \varepsilon_{eq}^p}{2} \right) \\ &= \frac{\Delta \sigma_{eq}}{2E} + \zeta \left[ \frac{\bar{\sigma}_y}{E} \left( n' \left( \frac{\Delta \sigma_{eq}}{2\bar{\sigma}_y} \right)^{\frac{1}{n'}} - n' + 1 \right) \right] \end{aligned} \quad (6)$$

where

$$\Delta \sigma_{eq} = \left( \frac{3}{2} \Delta S_{ij} \Delta S_{ij} \right)^{\frac{1}{2}} \quad (7)$$

$$\Delta S_{ij} = \Delta \sigma_{ij} - \frac{\Delta \sigma_{kk} \delta_{ij}}{3} \quad (8)$$

$$\zeta = \begin{cases} 0 & \text{for elastic cyclic loading} \\ 1 & \text{for elastic-plastic cyclic loading} \end{cases} \quad (9)$$

$\Delta \varepsilon_{eq}^e$  is the equivalent elastic strain range,  $\Delta \varepsilon_{eq}^p$  is the equivalent plastic strain range,  $\Delta \sigma_{eq}$  is the equivalent stress range,  $\Delta S_{ij}$  is the deviator stress range, E is Young's modulus,  $n'$  is the material cyclic strain-hardening exponent,  $\delta_{ij}$  is the Kronecker delta and  $\bar{\sigma}_y$  denotes the initial yield stress which is a material constant.

According to the deformation theory (Jhonson and Mellor, 1983) the relationship between the plastic components of multiaxial cyclic strain range and the deviator stress range can be written as:

$$\Delta \varepsilon_{ij}^p = \frac{3}{2} \frac{\Delta \varepsilon_{eq}^p}{\Delta \sigma_{eq}} \Delta S_{ij} \quad (10)$$

where  $\Delta \varepsilon_{ij}^p$  refers to the plastic components of multiaxial cyclic strain range.

Replacing for  $\Delta \varepsilon_{eq}^p$  in Eq. (10) from Eq. (6) then:

$$\Delta \varepsilon_{ij}^p = 3 \frac{\bar{\sigma}_y}{E} \left[ n' \frac{(\Delta \sigma_{eq})^{\frac{1-n'}{n'}}}{(2\bar{\sigma}_y)^{\frac{1}{n'}}} - \frac{n'-1}{\Delta \sigma_{eq}} \right] \Delta S_{ij} \quad (11)$$

Generally the total strain range  $\Delta \varepsilon_{ij}^t$  is the sum of the elastic and plastic strain range, i.e.

$$\Delta \varepsilon_{ij}^t = \Delta \varepsilon_{ij}^e + \zeta \Delta \varepsilon_{ij}^p \quad (12)$$

### 3.1 Proportional loading

Replace for  $\Delta \varepsilon_{ij}^e$  using generalized Hook's law

and for  $\Delta \varepsilon_{ij}^p$  from Eq. (11) in Eq. (12), the steady state cyclic stress-strain relationship for the multiaxial proportional loading is obtained as:

$$\begin{aligned} \Delta \varepsilon_{ij}^t &= \frac{(1+\nu)\Delta \sigma_{ij} - \nu \Delta \sigma_{kk} \delta_{ij}}{E} \\ &+ \zeta \left\{ 3 \frac{\bar{\sigma}_y}{E} \left[ n' \frac{(\Delta \sigma_{eq})^{\frac{1-n'}{n'}}}{(2\bar{\sigma}_y)^{\frac{1}{n'}}} - \frac{n'-1}{\Delta \sigma_{eq}} \right] \right\} \Delta S_{ij} \end{aligned} \quad (13)$$

where  $\nu$  is the Poisson's ratio.

In the new form of the multiaxial cyclic stress-strain relationship for proportional loading, the plastic component of the modified power law equation (Chu et al., 1993) have been modified and then it is combined with the elastic component. To the best of author's knowledge, this is an original work

The experimental results show that the cyclic hardening or softening of material is characterized by the expansion or contraction of the yield surface for multiaxial cyclic loading (Ellyin and Neale, 1979; Ellyn, 1987). Therefore, under multiaxial proportional loading, the relationship between the cyclic plastic strain range and the deviator stress range can be expressed as:

$$\Delta \varepsilon_{ij}^p = \phi(\Delta \sigma_{eq}) \Delta S_{ij} \quad (14)$$

where  $\phi(\Delta \sigma_{eq})$  is called yield surface function. It can be seen from Eqs. (12), (13) and (14) that the function  $\phi(\Delta \sigma_{eq})$  is:

$$\phi(\Delta \sigma_{eq}) = 3 \frac{\bar{\sigma}_y}{E} \left[ n' \frac{(\Delta \sigma_{eq})^{\frac{1-n'}{n'}}}{(2\bar{\sigma}_y)^{\frac{1}{n'}}} - \frac{n'-1}{\Delta \sigma_{eq}} \right] \quad (15)$$

Hence, multiaxial cyclic stress-strain relationship is related to the function  $\phi(\Delta \sigma_{eq})$ .

### 3.2 Nonproportional loading

The critical planes are defined as planes where a damage parameter will maximize. A class of damage parameters based on physical observations of crack initiation and growth are considered where their damage accumulation on the critical planes is used as fatigue failure criterion. The most popular critical plane is the one that takes shear strain as the damage parameter and is used here. The Brown-Miller and

Fatemi-Socie (Brown and Miller, 1973, Fatemi and Socie, 1988, Brown and Miller, 1982) used both the cyclic shear and normal strain (stress)  $\gamma_{max}$  and  $\epsilon_n$  on the plane of maximum shear, as the two basic fatigue damage parameters.

In the case of thin-walled tube under the tension-torsion multiaxial fatigue test schematically shown in Fig. 1, the state of strain will be:

$$\begin{aligned} \epsilon_{xx} &= \epsilon_a \sin \omega t, \quad \epsilon_a = \frac{\Delta \epsilon}{2} \\ \gamma_{xy} &= \gamma_a \sin(\omega t - \varphi), \quad \gamma_a = \frac{\Delta \gamma}{2} \end{aligned} \tag{16}$$

where  $\gamma_a$  and  $\epsilon_a$  are the applied torsion and tension strain amplitudes,  $\Delta \epsilon$  and  $\Delta \gamma$  are applied tension and torsion strain range, respectively and  $\varphi$  is the phase difference.

The critical plane is obtained by differentiating the shear strain on any plane of angle  $\alpha$ , as shown in Fig. 1, with respect to  $\alpha$  and setting it equal to zero to get (Kanazawa et al., 1977):

$$\alpha' = \frac{1}{4} \tan^{-1} \left( \frac{2 \frac{\gamma_a}{\epsilon_a} (1+\nu) \cos \varphi}{(1+\nu)^2 - \left(\frac{\gamma_a}{\epsilon_a}\right)^2} \right) \tag{17}$$

Then the maximum shear strain and the normal strain will be:

$$\gamma_{max}(t) = \gamma_{max} \sin \left[ \omega t + \tan^{-1} \left( \frac{\left[ \frac{-\gamma_a}{\epsilon_a} \cos 2\alpha' \sin \varphi \right]}{\left[ \frac{\gamma_a}{\epsilon_a} \cos 2\alpha' \cos \varphi - (1+\nu) \sin 2\alpha' \right]} \right) \right] \tag{18}$$

$$\epsilon_n(t) = \frac{1}{2} \epsilon_n \sin \left[ \omega t - \tan^{-1} \left( \frac{\left[ \frac{\gamma_a}{\epsilon_a} \sin 2\alpha' \sin \varphi \right]}{\left[ (1+\nu) \cos 2\alpha' + (1-\nu) + \frac{\gamma_a}{\epsilon_a} \sin 2\alpha' \cos \varphi \right]} \right) \right] \tag{19}$$

where

$$\begin{aligned} \gamma_{max} &= \epsilon_a \left\{ \left[ \frac{\gamma_a}{\epsilon_a} \cos 2\alpha' \cos \varphi - (1+\nu) \sin 2\alpha' \right]^2 \right. \\ &\quad \left. + \left[ \frac{\gamma_a}{\epsilon_a} \cos 2\alpha' \sin \varphi \right]^2 \right\}^{1/2} \end{aligned} \tag{20}$$

$$\begin{aligned} \epsilon_n &= \frac{1}{2} \epsilon_a \left\{ \left[ 2(1+\nu) \cos^2 \alpha' - 2\nu + \frac{\gamma_a}{\epsilon_a} \sin 2\alpha' \cos \varphi \right]^2 \right. \\ &\quad \left. + \left[ \frac{\gamma_a}{\epsilon_a} \sin 2\alpha' \sin \varphi \right]^2 \right\}^{1/2} \end{aligned} \tag{21}$$

and

$$\begin{aligned} -\frac{\pi}{2} &< \tan^{-1} \left( \frac{\left[ \frac{-\gamma_a}{\epsilon_a} \cos 2\alpha' \sin \varphi \right]}{\left[ \frac{\gamma_a}{\epsilon_a} \cos 2\alpha' \cos \varphi - (1+\nu) \sin 2\alpha' \right]} \right) \\ &+ \tan^{-1} \left( \frac{\left[ \frac{\gamma_a}{\epsilon_a} \sin 2\alpha' \sin \varphi \right]}{\left[ (1+\nu) \cos 2\alpha' + (1-\nu) + \frac{\gamma_a}{\epsilon_a} \sin 2\alpha' \cos \varphi \right]} \right) < \frac{\pi}{2} \end{aligned} \tag{22}$$

Jordan et al. (1985) and Wang-Brown (1993) have indicated that the shear strain  $\gamma_{max}$  and the normal strain excursion  $\epsilon_n^*$ , given as:

$$\begin{aligned} \epsilon_n^* &= \frac{1}{2} \Delta \epsilon_n \\ &\left\{ 1 + \cos \left[ \tan^{-1} \left( \frac{\left[ \frac{\gamma_a}{\epsilon_a} \sin 2\alpha' \sin \varphi \right]}{\left[ (1+\nu) \cos 2\alpha' + (1-\nu) + \frac{\gamma_a}{\epsilon_a} \sin 2\alpha' \cos \varphi \right]} \right) \right] \right. \\ &\quad \left. + \tan^{-1} \left( \frac{\left[ \frac{-\gamma_a}{\epsilon_a} \cos 2\alpha' \sin \varphi \right]}{\left[ \frac{\gamma_a}{\epsilon_a} \cos 2\alpha' \cos \varphi - (1+\nu) \sin 2\alpha' \right]} \right) \right\} \end{aligned} \tag{23}$$

are the two damage parameters that control multiaxial fatigue damage .

The equivalent strain range is given as (Shang and Wang, 1998):

$$\frac{\Delta \epsilon_{eq}}{2} = \left[ \epsilon_n^{*2} + \frac{1}{3} \left( \frac{\Delta \gamma_{max}}{2} \right)^2 \right]^{1/2} \tag{24}$$

where it is valid for both proportional and non-proportional loading cases. The modified strain-life relationship takes into account the effect of additional hardening under nonproportional loading and can be

used to calculate the equivalent stress amplitude  $\frac{\Delta\sigma_{eq}^{NP}}{2}$  for nonproportional loading case, i.e.

$$\frac{\Delta\epsilon_{eq}}{2} = \frac{\Delta\sigma_{eq}^{NP}}{2E} + \zeta \left[ \frac{\bar{\sigma}_y}{E} \left( n' \left( \frac{\Delta\sigma_{eq}^{NP}}{2\bar{\sigma}_y} \right)^{\frac{1}{n'}} - n' + 1 \right) \right]^\infty \quad (25)$$

The multiaxial equivalent cyclic stress-strain relationship for nonproportional loading case may be obtained by generalizing Eq. (25) as follows:

$$\frac{\Delta\epsilon_{eq}^{NP}}{2} = \frac{\Delta\sigma_{eq}^{NP}}{2E} + \zeta \left[ \frac{\sigma_y^{NP}}{E} \left( n'_{NP} \left( \frac{\Delta\sigma_{eq}^{NP}}{2\sigma_y^{NP}} \right)^{\frac{1}{n'_{NP}}} - n'_{NP} + 1 \right) \right] \quad (26)$$

where  $\sigma_y^{NP}$  and  $n'_{NP}$  are multiaxial cyclic yield strength and the strain hardening exponent under nonproportional loading, respectively.

Kanazawa (1979) showed experimentally that nonproportional loading has minor effect on the cyclic strain hardening exponent. Thus, it may be concluded that the only effect of nonproportional loading is on the material yield strength.

The cyclic stress-strain relationship for multiaxial nonproportional loading case can be obtained by generalizing Eq. (13) as follows:

$$\Delta\epsilon'_{ij} = \frac{(1+\nu)\Delta\sigma_{ij} - \nu\Delta\sigma_{kk}\delta_{ij}}{E} + \zeta \left\{ 3 \frac{\sigma_y^{NP}}{E} \left[ n' \frac{(\Delta\sigma_{eq}^{NP})^{\frac{1-n'}}{n'}}{(2\sigma_y^{NP})^{\frac{1}{n'}}} - \frac{n'-1}{\Delta\sigma_{eq}^{NP}} \right] \right\} \Delta S_{ij} \quad (27)$$

The new multiaxial cyclic stress-strain relationship for nonproportional loading is more practical and simple. To the best our knowledge, this new relationship has not been seen in the related existing papers.

The yield surface functions  $\phi(\Delta\sigma_{eq}^{NP})$  for nonproportional loading case can be written as follows:

$$\phi(\Delta\sigma_{eq}^{NP}) = 3 \frac{\sigma_y^{NP}}{E} \left[ n' \frac{(\Delta\sigma_{eq}^{NP})^{\frac{1-n'}}{n'}}{(2\sigma_y^{NP})^{\frac{1}{n'}}} - \frac{n'-1}{\Delta\sigma_{eq}^{NP}} \right] \quad (28)$$

If the yield surface function of nonproportional

loading is known, the multiaxial cyclic stress-strain relationship can be obtained under nonproportional loading.

It is seen from the above derivation, the given multiaxial cyclic stress-strain relation in this paper is simple, and all material constants can be obtained by the uniaxial fatigue experiments and some derivation. Therefore, it is convenient for engineering applications.

For thin-walled tubular specimens, under tension-torsion cyclic loading, the tensor of the strain is as follows:

$$\begin{bmatrix} \epsilon_a & \frac{1}{2}\gamma_a & 0 \\ \frac{1}{2}\gamma_a & -\nu\epsilon_a & 0 \\ 0 & 0 & -\nu\epsilon_a \end{bmatrix} \quad (29)$$

where  $\epsilon_a$  and  $\gamma_a$  are the components of the strain loading.

The tensor of the stress response is expressed as:

$$\begin{bmatrix} \sigma_a & \tau_a & 0 \\ \tau_a & 0 & 0 \\ 0 & 0 & 0 \end{bmatrix} \quad (30)$$

where  $\sigma_a$  and  $\tau_a$  are obtained from Eqs. (7), (8), (16) and (27):

$$\sigma_a = \frac{\epsilon_a}{\left\{ \frac{1}{E} + \frac{2\sigma_y^{NP}}{E} \left[ n' \frac{(\Delta\sigma_{eq}^{NP})^{\frac{1-n'}}{n'}}{(2\sigma_y^{NP})^{\frac{1}{n'}}} - \frac{n'-1}{\Delta\sigma_{eq}^{NP}} \right] \right\}} \quad (31)$$

$$\tau_a = \frac{\frac{\gamma_a}{2}}{\left\{ \frac{1+\nu}{E} + \frac{3\sigma_y^{NP}}{E} \left[ n' \frac{(\Delta\sigma_{eq}^{NP})^{\frac{1-n'}}{n'}}{(2\sigma_y^{NP})^{\frac{1}{n'}}} - \frac{n'-1}{\Delta\sigma_{eq}^{NP}} \right] \right\}} \quad (32)$$

## 4. Experimental verifications and discussion

### 4.1 Proportional loading

The process of estimating multiaxial cyclic stress-strain relationship under proportional loading is simple. For example, the various material constants of

uniaxial fatigue for SAE Steel 1045 are shown in Table 1. A proportional loading path of strain is shown in Fig. 2. The stress response values corresponding to all points on strain-loading path can be obtained. The

Table 1. Material parameters of Steel 1045.

$\bar{\sigma}_y$ [MPa]	380
$\sigma_{ut}$ [MPa]	621
$E$ [MPa]	204000
$\nu$	0.3
$n'$	0.208

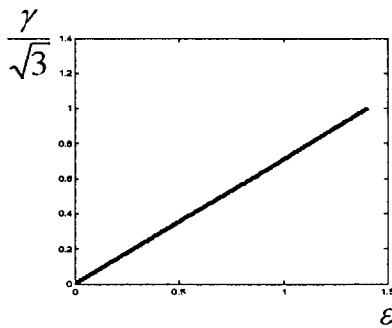


Fig. 2. Strain loading path “ $\epsilon - \frac{\gamma}{\sqrt{3}}$ ”.

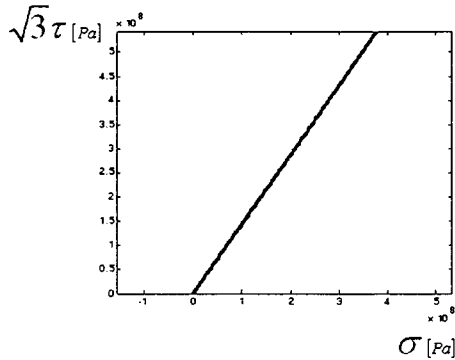


Fig. 3. Stress response “ $\sigma - \sqrt{3}\tau$ ”.

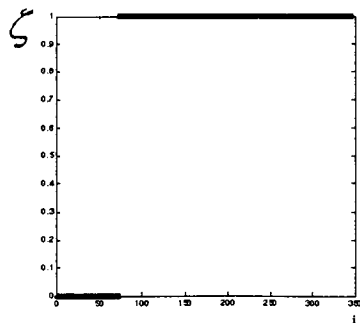


Fig. 4. Values of elastic-plastic coefficient versus number of steps i, with increments of  $\Delta\epsilon$ .

process of estimation is accomplished by means of computer (MATLAB Code). The estimation stress response “ $\sigma - \sqrt{3}\tau$ ” is shown in Fig. 3, which is an example of the computer printout and the components of stress response value are calculated by Eq. (13). Figure 4 displays the state of elastic-plastic coefficient “ $\zeta$ ” for strain loading path.

Note that for the in-phase (linear) strain path applied, as shown in Fig. 2, the resulting path in stress-space will be linear as shown in Fig. 3.

4.2 Nonproportional loading

The estimation steps of multiaxial cyclic stress-strain relationship under nonproportional loading are mainly illustrated. The applied loading is sinusoidal wave. The 90° out of phase nonproportional loading path is shown in Fig. 5. It is needed to estimate a stress response value corresponding to a certain point

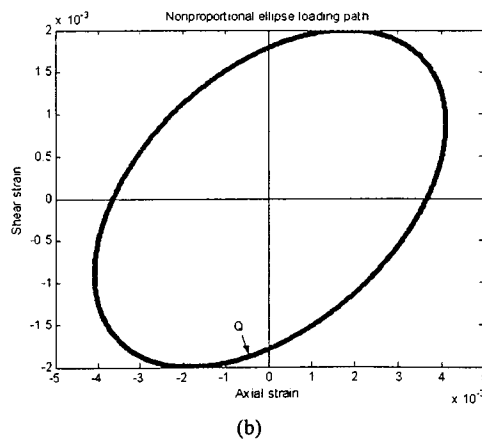
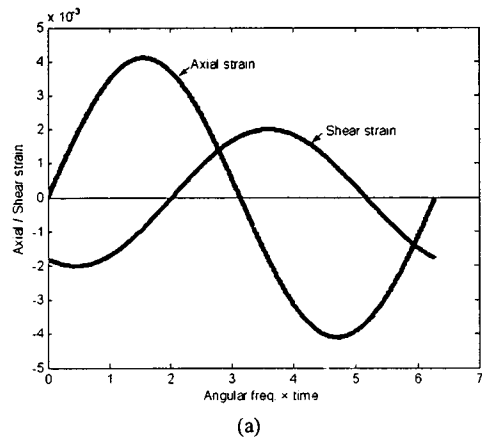


Fig. 5. The 90° out of phase nonproportional loading. (a) Axial / Shear strain shapes versus “angular freq. x time”; (b) The 90° out of phase nonproportional elliptical loading path.

Q on the strain-loading path. The procedure of the main process of estimation for multiaxial stress response is as follows:

1. Calculate the  $\alpha'$ ,  $\gamma_{\max}(t)$ ,  $\varepsilon_n(t)$ ,  $\varepsilon_n^*(t)$  and  $\frac{\Delta\varepsilon_{eq}}{2}$  by Eqs. (17), (18), (19), (23) and (24) respectively.
2. Find the maximum equivalent stress amplitude  $\left(\frac{\Delta\sigma_{eq}}{2}\right)_{\max}$  by Eq. (25) where  $\left(\frac{\Delta\sigma_{eq}}{2}\right)_{\max} \approx \left(\frac{\Delta\sigma_{eq}^{NP}}{2}\right)$
3. Determine a value of the multiaxial cyclic yield strength under nonproportional loading  $\sigma_y^{NP}$  by Eq. (26).
4. Compute the Equivalent strain amplitude  $\left(\frac{\Delta\varepsilon_{eq}^{NP}}{2}\right)_Q$  corresponding to point Q on the given loading path as shown in Fig. 5.
5. Determine a value of the equivalent stress amplitude  $\left(\frac{\Delta\sigma_{eq}^{NP}}{2}\right)$  on the stress response path corresponding to point Q of strain-loading path by Eq. (26).
6. Calculate the components of a stress response value in the point by Eqs. (30)–(32).
7. Choose the next point on the strain-loading path and to redo a process of estimation for multiaxial stress response from steps 4 to 6.

As stated above, the stress response values corresponding to all points on this strain-loading path can be worked out. The process of estimation accomplished by means of the computer (MATLAB Code).

In order to verify the multiaxial cyclic stress-strain relationship proposed in this paper, the 90° non-proportional strain-loading paths are employed to make the experimental verifications. Experimental data are taken from Refs. (Fatemi, 1989a) and (Fatemi, 1989b). Steel 1045 under 90° out-of-phase tension-torsion straining along strain paths at room temperature were used in this investigation. All specimens were thin-walled tube with 25.4 mm inside diameter and 2.54 mm wall thickness. The details of the experiments are given in Refs. (Fatemi, 1989a) and (Fatemi, 1989b). The loading strain shape was sinusoidal. The experimental and the estimated results are compared as shown in Fig. 6.

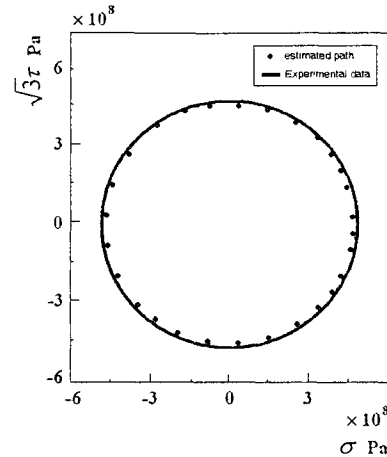


Fig. 6. Predicted and experimental stress response paths for thin-walled tubular specimen under the 90° nonproportional loading path.

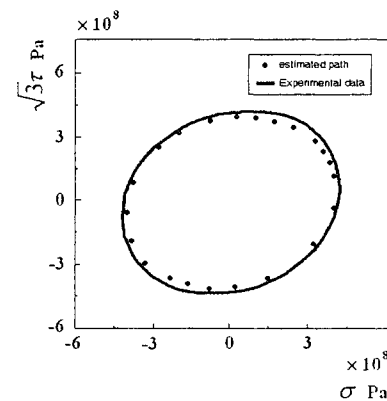


Fig. 7. Predicted and experimental stress response paths for thin-walled tubular specimen under the 45° nonproportional loading path.

The same method has also been applied to the 45° out of phase nonproportional elliptical loading path and the results are shown in Fig. 7.

As can be seen from these figures, for the sinusoidal strain history, the resulting stable stress paths for both the estimated and experimental results are circular and elliptical respectively. It can also be seen that a good agreement is observed, and it can satisfy the engineering demands.

In addition, the multiaxial cyclic yield strength behavior of the material and the additional cyclic hardening as a result of the out-of-phase straining can be studied.

It should be pointed out that the derived multiaxial cyclic stress-strain relationship in this paper is based on the material properties assumption of Massing. For

the other material properties, further modifications should be made. For the other types of specimens and test conditions, further studies and verifications are required.

## 5. Conclusions

The new steady state multiaxial proportional loading response has been derived. For the applied in-phase (linear) path, the resulting path in stress-space will also be linear. To consider the effects of the additional hardening due to the nonproportional loading, the normal strain excursion between two adjacent turning points of the maximum shear strain  $\Delta \varepsilon_n^*$ , and the maximum shear strain amplitude  $\gamma_{\max}$ , on the critical plane were combined as equivalent strain amplitude  $\Delta \varepsilon_{eq}^{cr}/2$ . The new obtained equivalent strain amplitude will replace the equivalent strain amplitude  $\Delta \varepsilon_{eq}/2$ , under proportional loading to study nonproportional loading. Therefore a new cyclic stress-strain relationship under multiaxial nonproportional loading has been derived in this paper. The given multiaxial cyclic stress-strain relationship under multiaxial nonproportional loading is simple and all material constants contained in multiaxial cyclic stress-strain relationship can be determined from a uniaxial test.

## Nomenclature

$\alpha$	: Angle of plane respect to axial load
$\alpha'$	: Angle of critical plane
$\alpha_{ij}$	: Back stress tensor
$\varepsilon$	: Axial strain
$\varepsilon_0$	: Reference axial strain
$\varepsilon_n$	: Normal strain to $\gamma_{\max}$ plane
$\varepsilon_n^*$	: Normal strain excursion between to turning point
$\Delta \varepsilon$	: Axial strain range
$\gamma$	: Shear strain
$\lambda$	: Material constant
$\lambda'$	: Cyclic coefficient
$\Delta \gamma$	: Shear strain range
$\varphi$	: Phase difference
$\sigma$	: Axial stress
$\sigma_0$	: Reference axial stress
$\bar{\sigma}_y$	: Yield strength (0.2%)
$\sigma_u$	: Ultimate strength
$\Delta \sigma$	: Axial stress range
$\tau$	: Shear stress
$\nu$	: Poisson's ratio

$\omega$	: Angular frequency
$E$	: Modulus of elasticity
$f$	: Yield function
$g$	: A function relating plastic strain
$n$	: Hardening exponent
$n'$	: Cyclic hardening exponent
$S_{ij}$	: Deviator stress
$\Delta S_{ij}$	: Deviator stress range
$t$	: Time

## Subscripts and superscripts

$eq$	: Equivalent quantities
$e$	: Elastic quantities
$p$	: Value connected with the plastic limit load
$ij$	: Component of tensor in $i$ th row, and $j$ th column
$NP$	: Nonproportional loading
$cr$	: Critical quantities
$\max$	: Maximum quantities

## References

- Bannantine, J. A., 1989, "A Variable Amplitude Multiaxial Fatigue Life Prediction Method," Report No. 151/UILU-ENG 89-3605 University of Illinois October.
- Brown, M. W. and Miller, K. J., 1973, "A Theory for Fatigue Under Multiaxial Stress-strain Condition," *Proceedings of the Institute of Mechanical Engineers*, Vol. 18, pp. 745~756.
- Brown, M. W. and Miller, K. J., 1982, "Two Decades of Progress in the Assessment of Multiaxial Low-cycle Fatigue Life," *ASTM STP 770*, pp. 482~499.
- Chu, C. C., 1984, "A Three-dimensional Model of Anisotropic Hardening in Metals and its Application to the Analysis of Sheet Metal Formability," *J. the Mechanics and Physics of Solids*, Vol. 32, pp. 197~212.
- Chu, C. C., Conle, F. A. and Bonnen, J. J. F., 1993, "Multiaxial Stress-strain Modeling and Fatigue Life Prediction of SAE Axle Shafts," *Advances in Multiaxial Fatigue ASTM STP 1191*, Philadelphia, pp. 37~54.
- Doong, S. H. and Socie, D. F., 1991, "Constitutive Modeling of Metals Under Nonproportional Cyclic Loading," *ASME J. Engng Mater Tech*, Vol. 113, pp. 23~30.
- Ellyin, F. and Neale, K. W., 1979, "Effect of Cyclic Loading on the Yield Surface," *ASME J. Pressure Vessel Tech*, Vol. 101, pp. 59~63.
- Ellyin, F., 1987, "A Cyclic Constitutive Relation for



Multiaxial Stress States," *The Second Inter. Conf. on Low Cycle Fatigue and Elasto-plastic Behavior of Materials*, Munich, K T Rice Editor, pp. 165~169.

Fatemi, A. and Socie, D. F., 1988, "A Critical Plane Approach to Multiaxial Fatigue Damage Including Out-of-phase Loading," *Fatigue and Fracture of Engineering Materials and Structures*, Vol, 11, No. 3, pp. 149~166.

Fatemi, A., 1989a, "Biaxial Fatigue of 1045 Steel Under In-phase and 90 Deg Out-of-phase Loading Conditions," *SAE AE-14 ISBN 0-89883-780-4*, pp. 121~137.

Fatemi, A., 1989b, "Cyclic Deformation of 1045 Steel Under In-phase and 90 Deg Out-of-phase Axial-torsion Loading Conditions," *SAE AE-14 ISBN 0-89883-780-4*, pp. 139~147.

Jhonson, W. and Mellor, P. B., 1983, "Engineering Plasticity," Ellis Horwood.

Jordan, E. H., Brown, W. M. and Miller, K. J., 1985, "Fatigue Under Severe Nonproportional Loading Multiaxial Fatigue," *ASTM STP853*, pp. 569~585.

Kanazawa, K., Miller, K. J. and Brown, M. W., 1977, "Low Cycle Fatigue Under Out-of-phase Loading Conditions," *J. of Engineering Materials and Technology ASME Transactions*, Vol. 99, pp. 22~28.

Kanazawa, K., Miller, K. J. and Brown, M. W., 1979, "Cyclic Deformation of 1% Cr-Mo-V Steel Under Out-of-phase Loads," *Fatigue Engng Mater Struct*, Vol. 2, pp. 217~222.

McDowell, D. L., 1985, "A Two-surface Model for Transient Nonproportional Cyclic Plasticity," *J. Applied Mechanics*, Vol, 52, pp. 298~308.

McDowell, D. L., Socie, D. F. and Lamba, H. S., 1982, "Multiaxial Nonproportional Cyclic Deformation," *Low-cycle Fatigue and Life Prediction, ASTM STP770*, pp. 500~518.

Mroz, Z., 1967, "On the Description of Anisotropic Work-hardening," *J. the Mechanics and Physics of Solids*, Vol. 15, pp. 163~175.

Shang, D. G. and Wang, D. J., 1998, "A New Multiaxial Fatigue Damage Model Based on the Critical Plane Approach," *In. J. Fatigue*, Vol, 20, No. 3, pp. 241~245.

Socie, D., 1993, "Critical Plane Approaches for Multiaxial Fatigue Damage Assessment," *Advances in Multiaxial Fatigue. ASTM STP 1191*, Philadelphia, pp. 7~36.

Wang, C. H. and Brown, M. W., 1993, "A Path-independent Parameter for Fatigue Under Proportional and Nonproportional Loading," *Fatigue Fract Engng Mater Struct*, Vol. 16, No. 1, pp. 1285~1298.